Cadmium sulphide / Zinc sulphide quantum dot decoration of three-dimensional porous graphene

Shibbir Ahmed

Department of Physics
Umeå Universitet
901 87 Umeå, Sweden

Master's thesis, 30 ECTS

Supervisors

Dr. Thomas Wågberg
Associate Professor
Department of Physics
Umeå University, Sweden

Dr. Guangzhi Hu
Research Engineer
Department of Physics
Umeå University, Sweden

Examiner

Dr. Magnus Andersson
Associate Professor
Department of Physics
Umeå University, Sweden

To my beloved parents and brother

Abstract

Graphene, a monolayer of graphite, has appeared as one of the most fascinating materials of today's Material Science research. The properties of graphene (GR) with high electronic conductivity, extraordinary strength and interesting chemical characteristics make it suitable for many different applications. All these tremendous properties of GR are relevant at the nanoscale, hence, in a view to exploit all these extraordinary properties in macroscopic applications, here, three dimensional (3D) porous structure of reduced graphene oxide (rGO) has been produced by chemical reduction at 90 °C under atmospheric pressure in a solution based process. Quantum dots (QDs) have been widely explored due to their excellent characteristics and the possibilities to tune the optical and electronic properties by controlling their size and structure, as well as their efficient multiple charge-carrier generations. In order to manufacture new nanostructures with low electron-hole recombination, and fast electron-transfer to improve the photovoltaic performance, QDs have been attached homogeneously with rGO sheets in 3D rGO. Alongside with the chemical reduction P^H values of GO aqueous suspension were also controlled to produce uniformly QDs decorated 3D rGO. No high pressure or chemical or physical cross-linkers are required in this simple synthesis method to produce QDs decorated 3D rGO with high mechanical strength. Influence of different washing solvent on QDs decoration in 3D rGO has also been analyzed. Decoration of QDs on rGO sheets, their size, crystal structure, and internal structure of QDs decorated 3D rGO were analyzed by Transmission Electron Microscopy (TEM), Scanning Electron Microscopy (SEM) and X-ray diffraction (XRD). This 3D architecture of rGO comprised with uniformly QDs decorated GR can be applied in various field because of its combined unique characteristics, for example, multiple charge-carrier generation, electron-hole separation, being light weight, porosity and fast transportation of charge.

Table of Contents

1. Introduction

In recent years, graphene (GR) has been implemented in numerous applications, such as, photovoltaic devices, sensors, supercapacitors, transistors, and electronics, owing to its extended sp^2-hybrid carbon network, two dimensional morphology, extremely large surface area, and superior electrical conductivity [1-7]. In particular, GR possess zero band gap and high electron mobility ($15000 cm^2 V^{-1} s$) [8] thus, GR has been largely regarded as a promising candidate for electron-acceptor and electron transport matrices [9]. Moreover, under certain conditions, integration of GR in photovoltaic device can enhance charge separation and facilitate charge-transport, and thereby improve the photovoltaic performance drastically [10]. As intrinsic stacked GR is a zero-gap semiconductor, or semi-metal, consequently electrons and holes in GR prefer to recombine and then quench quickly [10]. It occurs because in a semi-metal there is a very small overlap between the bottom of the conduction band and the top of the valance band. Consequently, there is no band gap and since Fermi level lies at least in one band and due to the negligible density of state at Fermi level the amalgamation of GR directly as an active layer into photovoltaic devices cannot assist electron-hole separation, and it also cannot help to improve the device performance [10].

Certainly, the above mentioned excellent properties of individual GR sheets are relevant at the nanoscale. In order to utilize the advanced properties for macroscopic applications, it is necessary to integrate individual two dimensional GR sheet into three dimensional (3D) functional architecture [11]. 3D architectures built from components of GR materials with inter-connected micropores and mesopores have drawn much attention for their various attractive properties, such as being light-weight and having high porosity, high electric conductivity, and large surface area [12]. The practical application of 3D structures comprising rGO is vast, and could potentially be applied in many areas such as sensors, supercapacitors, microelectromechanical system, catalytic electrode, and environmental applications [13-18].

When electrons and holes (charge carriers) are confined by potential barriers to small regions of space, and when the dimensions of the confinement are smaller than the de Broglie wavelength of the charge carriers; then semiconductors show extraordinary interesting characteristics rising from quantization effects. Similarly, semiconductor nanocrystals with diameter smaller than twice the exciton Bohr radius of bulk materials, also exhibit similar quantization effects [19]. Usually these effects start to take place in nanocrystal when the length range is less than about 25 to 10nm depending on the effective masses of the charge carriers. Studies have revealed that the electron effective mass in quantum dots is generally larger than the bulk value and it becomes anisotropic in dots with large aspect ratio [20]. When quantization effects become important for the nanoparticles they are usually referred to as quantum dots [19].

Due to the above characteristics and the possibilities to tune the optical and electronic properties of semiconductor nanoparticles (NPs), for example QDs, by controlling their size and structure, as well as their efficient multiple charge-carrier generations, this material have been considered as an attractive candidates for photoelectric applications [10]. However, in the case of manufacturing high-performance photoelectric devices with NPs, efficient electron-hole dissociation, as well as electron collection by the acceptor are the challenging issues that have not been addressed yet [10]. Nanocomposites of rGO and semiconductor NPs can be constructed to overcome the intrinsic properties of GR and shortcomings of semiconductor NPs; hence a new nanostructure is manufactured with low electron-hole

recombination, and fast electron-transfer, that would ultimately improve the photovoltaic performance [10]. With this in mind, several reports have been published regarding semiconductor NPs assembled on GR matrices. However, to the best of the author's knowledge, no report has been published so far regarding semiconductor NPs that is decorated in 3D porous rGO. Furthermore, studies in this particular area are of much interest since aggregation of NPs into larger complex is quite challenging. These challenges eventually present exciting scientific and engineering issues in designing such composites [4].

To utilize the outstanding nanoscale phenomena and transfer that into macroscopic applications, self-assembly has been widely accepted as one of the most efficient technique, which enables the integration of different nanosized materials into macroscopic devices [21]. Recently, significant progress has been made in the assembly of nanostructured materials [22] into 3D architecture, by following several processes; for example, *in situ* self-assembly [23], Langmuir-Blodgett assembly and the hydrothermal method [24]. Among various techniques; self-assembly of graphene oxide (GO) by a classical hydrothermal method was an efficient technique for making 3D macro-porous rGO structure [21]. In the hydrothermal process, the partially reduced GO agglomerate into 3D structures because of the strong attraction forces between the rGO sheets, owing to the van der Waals force, π-π stacking as well as plentiful of hydrogen bond of water [25]. In order to produce 3D structure of rGO this strategy has been tested to be efficient for the synthesis and application of GR supported 3D materials [26]. 3D architecture of GR was prepared by Shi *et al*. and applied as supercapacitor with good electrochemical behavior and high mechanical strength; this light-weight 3D structure of GR can support many times higher than its own weight [27].

Since the major component inside the macro-porous 3D structure of rGO produced by the hydrothermal method is water, the most dominant force of forming the 3D structure is the hydrogen bond [27]. In addition, to remove the water, freeze drying is a common method, however this method suffers from the fact that during the expansion of ice, the porous structure is damaged which induces negative consequences for the mechanical strength of 3D reduced graphene [28]. In this respect, a homogeneous and uniform decoration of QDs in the 3D rGO structure will not only facilitate the electron hole dissociation, but also protect the porosity and enhance the mechanical stability of 3D rGO, by adding an extra component to stabilize the structure.

This thesis report focuses however primarily on the decoration process of CdS QDs in porous 3D rGO structure by the hydrothermal reduction methods. Here it is important to note that most methods are reported for CdS, which possess excellent electronic properties as QDs, but due to the severe health threats of Cadmium [29], the author have chosen to mainly focus on processes that involves ZnS NPs on rGO sheets. Furthermore, this thesis not only focuses on the decoration of QDs in 3D rGO but also on the maintaining of high mechanical strength of QDs decorated 3D rGO. The mechanism and the reactants involved in the synthesis process which has strong impact on the mechanical strength of QDs decorated 3D rGO has been also identified, and then those factors were applied properly to obtain homogeneously decorated QDs in 3D rGO with high mechanical stability. Since, it is very important to remove all unwanted by products from QDs decorated 3D rGO therefore it was washed with different solvent and the effect of washing solvent on attachment of QDs with rGO has been examined.

In this thesis work I have tried two synthesis procedures. The first process is based on a one-step synthesis where the production of QDs and the anchoring of these QDs in 3D rGO are made simultaneously; while in the second method the QDs are first produced separately

followed by an anchoring process on the rGO in 3D rGO. Although the one-step process would be highly desirable, it has many drawbacks making it difficult to realize experimentally. Some success in these aspects could be gained by controlling the p^H values of GO suspension. Finally, by numerous attempts and by testing a large number of different synthesis conditions, (of which not all details will be reported here to save readers time) I have been able to homogeneously decorate well dispersed ZnS QDs onto rGO in a 3D rGO structure. It is also found that the decoration of ZnS QDs on rGO in 3D rGO is not only homogeneous but we also show that the produced 3D rGO is porous, light weight and exhibits high mechanical strength. The anchoring process has been analyzed and investigated by a number of different techniques, such as electron microscopy, thermo gravimetric analysis, optical absorption, x-ray diffraction and electron diffraction.

2. Theory

A GO sheet is considered as a single-layer of graphite, where different hydrophilic functional groups are attached. Fig. 1 shows the hydrophilic carboxyl groups (red colored) together with hydroxyl and epoxy groups (blue colored) in the single-layer of graphite [30-32]. Such functional groups play an important role for the dispersibility of GO by producing electrostatic repulsions between ionized functional groups which hinders the aggregation of GO sheets and thus allows for GO to form stable colloidal dispersions in aqueous solutions [33]. Moreover, due to the functional groups the reduced GO (rGO) is often corrugated and wrinkled which hampers the re-stacking of rGO [34]. By reducing the GO, many of the functional groups are removed and the low electric conductivity of GO can be increased significantly, and therefore a controlled reduction process is an efficient way to gain desirable electrical properties of this material [35].

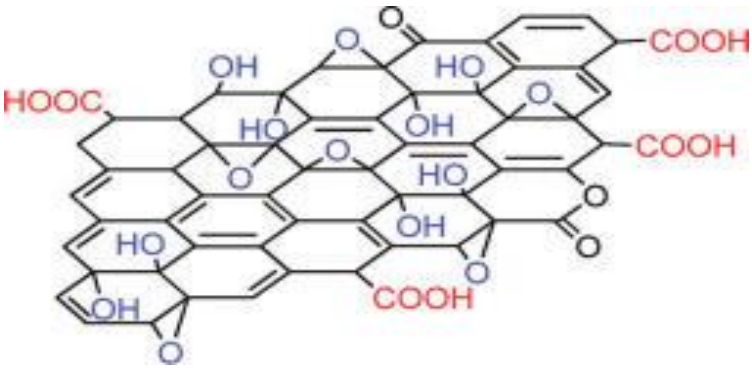

Fig. 1 Chemical structure of GO [30-32].

Micromechanical exfoliation of bulk graphite was one of the standard techniques used initially to obtain GR [2]. It is possible to produce high-quality GR with superior structure by this process; however it is not suitable for large-scale applications in future. Motivated by the pioneering work on GR, and the necessity for having big amounts of GR, several alternative reliable synthetic routes have been developed. These can be categorized as bottom-up and top-down approaches [36]. Epitaxial growth [37], chemical vapor deposition (CVD) [38], and segregation growth [39] are examples of top-down approaches, and by these methods high quality GR for optoelectronic application can be produced. The top-down approaches include exfoliation of graphite via sonication [40] and wet chemical methods [41, 42] which can be simply scaled up at low cost. The production of GR materials by oxidation-exfoliation-reduction of graphite powder (in Fig. 2) has attracted most interest compared to other methods due to its exclusive advantages, such as high production capability, simple functionalization and tunable characteristics of GR materials, and easy of application in solution without the

requirement of special equipment [41]. Fig. 2 demonstrates the synthesis route of GO by exfoliation of graphite oxide prepared by chemical oxidation of graphite powder with strong oxidants in acidic media.

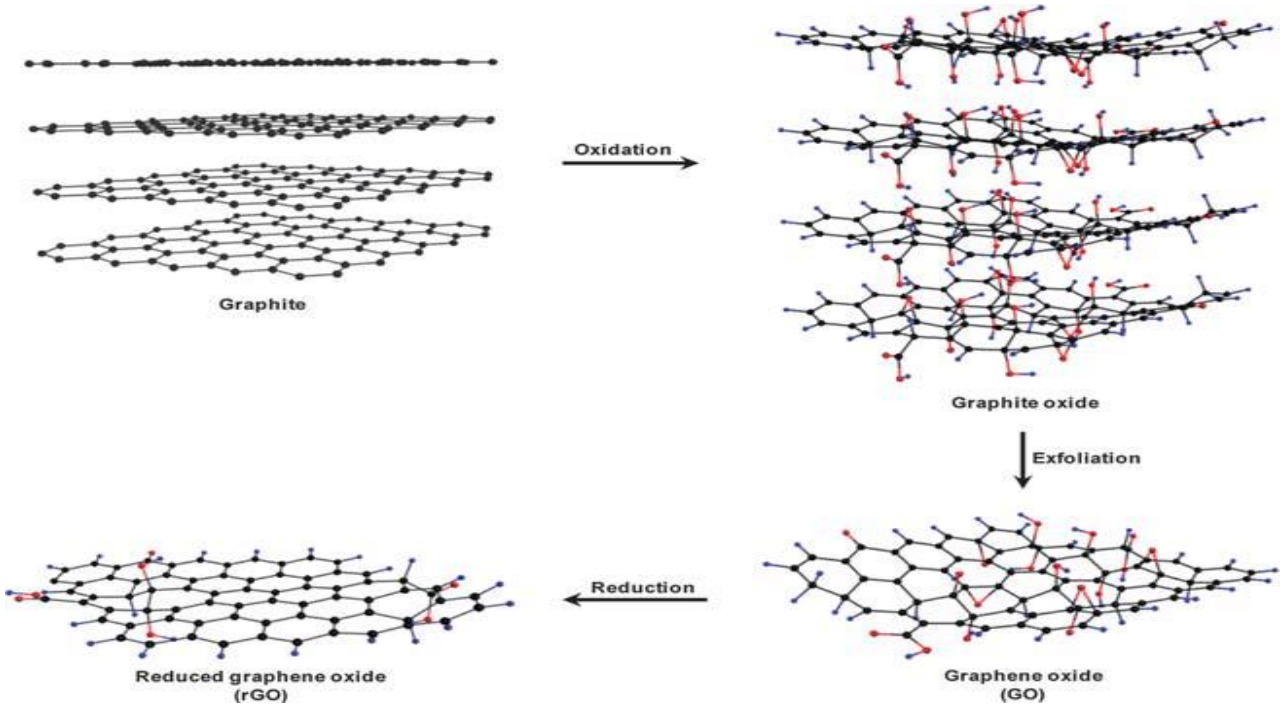

Fig. 2 Schemetic showing of the preparation of chemically modified graphene where graphite as starting materials [43].

In this study GO was prepared by Hummers method where ultra-pure graphite is strongly oxidized into graphite oxide creating functional groups distributed across the carbon skeleton. This increases the inter layer spacing and the van der Waals force between adjacent layers becomes weakened. As previously mentioned the functional groups helps to make the GO dispersible in water. This process can be facilitated by strong sonication leading to a dispersion stabilized by the mutual electrostatic attraction and repulsion of the GO flakes (Fig. 3) [33].

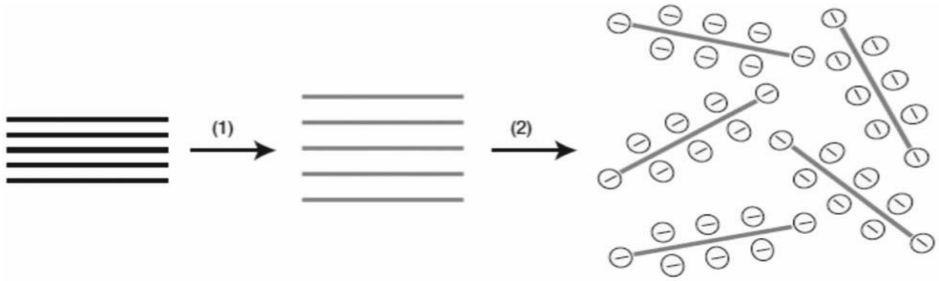

Fig. 3 Chemical route to the synthesis of aqueous GO suspension. (1) Black blocks showing oxidation of graphite to graphite oxide (lighter colored blocks) with enhanced inter layer spacing. (2) Stabilized GO suspension in water due to electrostatic repulsion after strong sonication [33].

In a three dimensional architecture of rGO (in Fig. 4) graphene becomes more active with more functions owing to repaired aromatic structure and better conductivity compared to GO [36]. Self-assembly of the rGO *in situ* in water or oganic solvents is the simplest way to produce 3D rGO architecture [36]. The van der Waals force between the graphene basal

planes increases due to the reduction of GO which lead to rGO precipitaion or gelation [36]. The gelation of rGO is controlled by the force balance between electrostatic repulsion and inter-planer van der Waals interaction [36]. Becasue of the abundent hydrophilic groups and strong electrostatic repulsion effect, two dimensional GO sheets were randomly dispersed in water before the reduction [36]. Moreover, when GO sheets are hydrothermally reduced, their basal planes become hydrophobic because of the elimination of hydroxyl and epoxy groups and restroing conjugated domains, which causes to a three dimensional arbitrary stacking between flexible graphene sheets [36]. By hydrothermal reduction method; when the GO concentartion is high enough, the *in situ* formed rGO can be assembled into 3D network with pore sizes ranging from sub-micrometer to several micrometer [36].

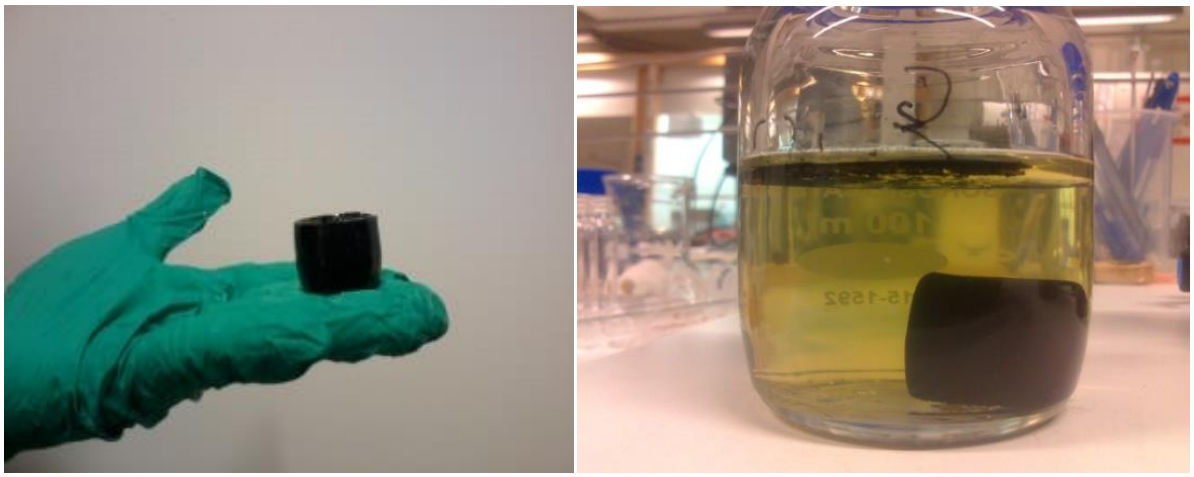

Fig. 4 3D structure of QDs decorated porous rGO.

Same as the hydrothermal approach; chemical reduction of GO increases the hydrophobic and Π-Π interaction between graphene sheets which leads to their self-assembly to a 3D structure with pore sizes ranging from sub-micrometer to several micrometers [36]. To produce the 3D graphene architecture via the *in situ* self-assembly of rGO produced by chemical reduction method, various types of reductants such as Na_2S, $NaHSO_3$, hyroquinone and HI have been witnessed to be used [23]. Furthermore, study has also revealed that 3D architecture of graphene is produced via the *in situ* self-assembly of graphene made by easy chemical reduction at 95°C under atmospheric pressure without shaking, and where chemical or physical cross-linkers or high pressures are not required [23].

In addition, the aggregation of additive free GO can be controlled by the tuning of p^H value, bacasue acidification of GO dispersion would weaken the electrostatic replusion which helps to the production of GO flocculent [44]. GO solution is acidic when p^H value is 4.6 and if the p^H is lower than 4.6 then the aggregation gets faster, and if the p^H value goes higher than 4.6 the repulsion forces between GO sheets would increase [44]. Moreover, pure hydrogel of GO can also be prepared by ultrasonication becasue sonication breaks the GO sheets into smaller pieces, displaying new sheet edges without stabilizing carboxyl groups, and it is this alter in surface chemistry that helps to gelation [45].

In this study quantum dots were produced in solution by a classical wet chemistry method. The as produced QDs were attached with rGO sheets in porous 3D rGO structure without any assistance of cross linkers, because if any cross linker is used they could affect in several ways such as, they could make a shield outside the QDs which could hamper the charge dissociation, they also could produce repulsive force between the individual rGO sheets which

could hamper the production of 3D porous architecture of rGO. Formation of QDs in this synthesis process has been illustrated by following reactions.

$$CdCl_2 + Na_2S = CdS\ (QDs) + 2NaCl$$
$$Cd(Ac)_2 + Na_2S = CdS\ (QDs) + 2NaAc$$
$$Zn(Ac)_2 + Na_2S = ZnS\ (QDs) + 2NaAc$$

Na_2S was utilized in this synthesis because it not only helps to produce QDs in solution but also as a strong reducing agent it helps to reduce the GO in solution to make 3D porous architecture.

Photo generated electrons and holes are created with excess energy in bulk semiconductor if the energy of photon absorbed in it is greater than the band gap energy, these energetic electron-hole pairs are called hot carriers in bulk semiconductor. Similarly, in QDs excitons with excess energy are created if the energy of the photon absorbed in it is greater than the lowest energy excitonic transition, these are termed hot excitons because electrons and holes are coupled by confining them in small volume in QDs [19]. QDs has attracted much interest because it has been foretold that slow cooling of energetic electron can arise in QDs at low photo generated carrier densities, explicitly at light intensities corresponding to the solar isolation on earth [19]. In bulk semiconductor, the generation of more than one electron-hole pairs by a single photon absorption has been known for over 50 years; it has been noticed in the photocurrent of bulk p-n junctions in Ge, PbS, Si, PbSe, InSb, and PbTe, and this system is called *impact ionization* [19]. However, this production of more than one electron-hole pairs by a single photon absorption cannot contribute to improved quantum yields (QY) in present solar cells fabricated by bulk Si, CdTe, $CuIn_xGa_{1-x}Se_2$, or III-V semiconductors since the highest QY for *impact ionization* does not generate extra electron-hole pairs until photon energy reach the ultraviolet region of the spectrum [19].

Furthermore, the threshold photon energy for *impact ionization* in bulk semiconductor exceeds that essential for energy conservation alone because crystal momentum (**K**) must also be conserved [19]. The *impact ionization* rate must compete with the rate of energy relaxation by phonon emission through electron-phonon scattering, and it has been observed that when the kinetic energy of the electron is many multiples of the band gap energy (E_g) only then the rate of *impact ionization* becomes competitive with phonon scattering rates [19]. Moreover, among others Si is one of the widely used materials in present photovoltaic cells where the *impact ionization* does not become high if the incident photon energy does not exceed 3.5 eV, an ultraviolet energy threshold above which the existence of the photons in the solar spectrum is less than 1%. Photons with energies ranging from about 0.5 to 3.5 eV existing in the solar spectrum [46], hence, in the bulk semiconductor *impact ionization* is not an efficient approach to increase efficiency of the photovoltaic cells [19].

On the other hand, in quantum dots due to carrier confinement and the concurrently increased electrons-holes coulomb interactions, the rate of Auger processes, including the inverse Auger process of multiple exciton generation (MEG) can be significantly increased, and MEG occurs very fast; it has been shown to be less than 100fs [19]. The MEG in QDs becomes efficient because of the ultrafast MEG rate and that is much faster than the hot exciton cooling rate created by electron-phonon interactions [19]. In addition, crystal momentum is not a good quantum number for three dimensionally confined carriers because according to the Heisenberg Uncertainty Principle the well-defined location of the electrons and holes in the nanocrystal makes the momentum uncertain [46]. Since, in quantum dots the crystal momentum is not a good quantum number and momentum need not to be conserved; so the threshold photon energy for the system to produce two electron-hole pairs by a single photon

can approach values as low as twice the threshold energy for absorption [19]. The solar spectrum supply more photons to the effect in materials with ideal band gaps after lowering the threshold [19]. This concept has been shown below in Fig. 5.

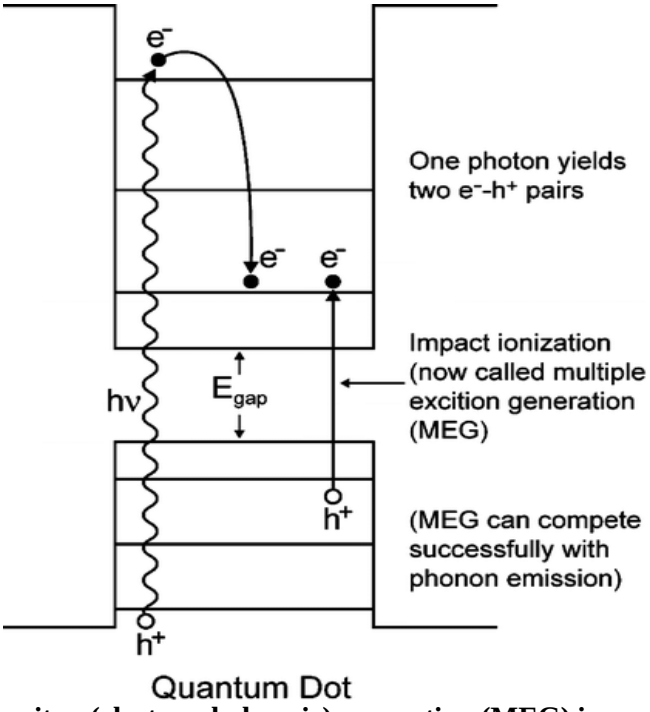

Fig. 5 Multiple exciton (electron-hole pair) generation (MEG) in quantum dots [47].

Moreover, in semiconductor quantum dots the rate of cooling of photo excited excitonic states compared to cooling through phonon emission dominates the efficiency of MEG [46]. In the quantized semiconductor structures, the rate of excited state exciton cooling can be slowed down because of the presence of discrete quantized energy levels [46]. The reasons behind this slowed cooling is that the energy separation between quantized levels in QDs can be several times the typical phonon energy, and if high energy electrons and holes in higher excited state want to be cooled by relaxing from a given quantum level to the next lower level then many phonon need to be emitted simultaneously via electron phonon scattering to satisfy energy conservation [46]. This necessitates concurrent multi-particle scattering events which become extremely impossible with increasing numbers of phonons emitted [46]. This effect is named a 'phonon bottleneck', and it has been experimentally proved with InP quantum dots the cooling time of hot electrons increased by about a factor of 10 if the Auger cooling path is blocked, this become possible if the photo generated holes is removed very quickly or avoiding their generation in the first place by injecting only electron into the QDs [48].

3. Experimental approach

3.1 Materials

To produce QDs decorated porous 3D rGO; following essential materials were utilized.

1. GO (Produced by Hummer method).
2. Cadmium chloride ($CdCl_2$).
3. Sodium sulfide (Na_2S).
4. Ethanol (C_2H_5OH) (99.5%).
5. Benzyl mercaptan (BM).
6. Dimethyl sulfoxide (DMSO).
7. Cadmium acetate dihydrate ($Cd(CH_3COO)_2.2H_2O$).
8. Zinc acetate dihydrate ($Zn(CH_3COO)_2.2H_2O$).
9. n-dodecyl sulfide.
10. Distilled water.
11. Ammonium solution (30%).
12. Acetone.

It is to be noted that all the above mentioned chemicals were utilized as received without any further purifications.

3.2 Synthesis: Decoration of QDs in 3D reduced graphene oxide

Decoration of QDs in 3D rGO was carried out by 6 different methods. All of these methods are schematically illustrated by 4 schemes. Method 1, 2, and 3 are demonstrated by the scheme in Fig. 6a below. Method 4 and method 5 are illustrated by scheme in Fig. 6b and in Fig. 6c below respectively. Method 6 was the most successful process and is demonstrated by scheme 6d below.

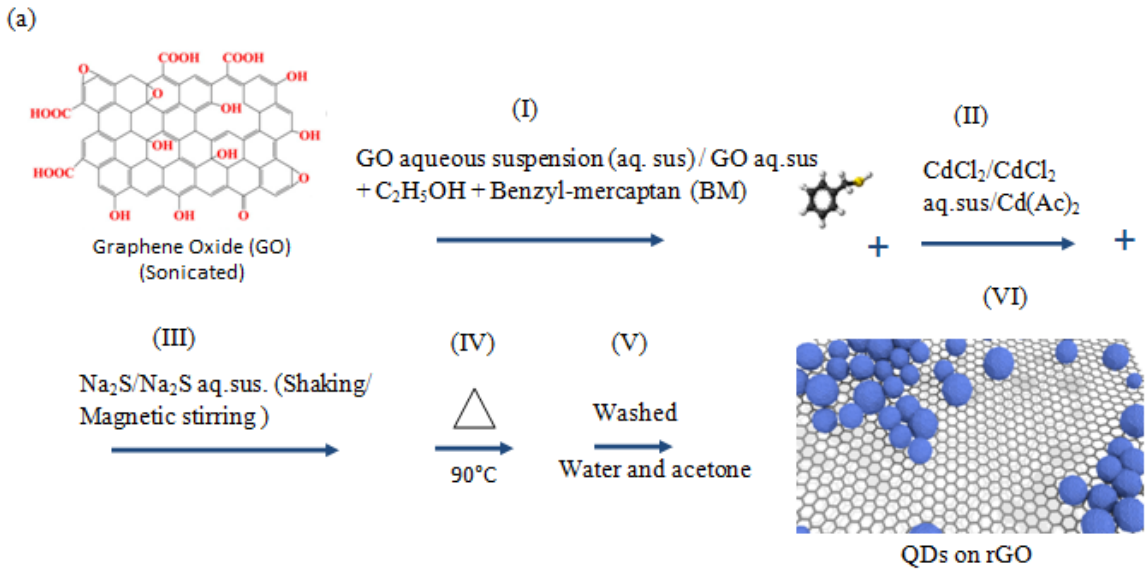

Fig. 6(a) QDs decorated 3D rGO synthesis scheme illustrates the process where decoration of QDs and production of 3D rGO occur simultaneously.

Method 1 - One-step method with the impact of weight ($CdCl_2$), magnetic stirring, sonication, and position of QDs in 3D rGO

In this approach, GO was reduced to produce 3D porous rGO structure by chemical reduction method in water solution and Na_2S was used as a strong reducing agents. To produce quantum dots in this solution and to get them attached with rGO sheets in 3D porous rGO structure $CdCl_2$ was added into this process. It was also examined how the production of quantum dots are varying with the various amount of $CdCl_2$. Four clean bottles were taken and 60ml of GO water solutions (0.001g GO/1ml water) was taken into each bottles and 30 minutes strong sonication was given (Fig. 6a step-I). 1mg, 2mg, 10mg and 20mg $CdCl_2$ were added into different bottles respectively (Fig. 6a step-II). Each bottle was given 10 minutes strong sonication after adding $CdCl_2$. 0.3g Na_2S was added into each bottle and was shaken about three minutes (Fig. 6a step-III). The four bottles were then kept in the oven at 90°C for about 6 hours under atmospheric pressure (Fig. 6a step-IV). After one and half hours the solution started to show sign of agglomeration giving a 3D structure of rGO. After 6 hours bottles were taken out from the oven and nice 3D structure of rGO was formed. Sample was washed three times separately with distilled water and then with acetone (Fig. 6a step-V) with 5 minutes sonication. After that sample was precipitated by performing 10 minutes centrifugation at each time of washing.

In order to act effectively in the reaction, in this attempt Na_2S aqueous solution was added in the reaction instead of using solid form of it. Produced 3D rGO was given strong sonication and magnetic stirring at the time of washing to observe the effect of strong sonication and magnetic stirring on the decoration and attachment of NPs on rGO. 60ml GO water solution (0.001g GO/1ml water) was taken and 30 minutes strong sonication was given and then, the solution was taken into a bottle. 20mg $CdCl_2$ was mixed into this solution. 0.3g Na_2S was mixed with 4ml of water in another small bottle and shaken strongly to dissolve it perfectly. This Na_2S solution was added to the first bottle drop by drop at rate of 1 drop/sec under simultaneous shaking (Fig. 6a step-III). The bottle was then kept in the oven at 90°C under atmospheric pressure and precipitation was started after one and half hours. After 6 hours bottle was taken out from the oven and 3D porous structure of rGO was formed nicely. Sample was washed three times with water and acetone but this time some sample was sonicated 5 minutes and some sample was stirred 5 minutes by magnetic stirrer at each time of washing instead of sonication (Fig. 6a step-V). Sample was collected by performing 10 minutes centrifugation at each time of washing.

It is known that that if the amount of $CdCl_2$ is increased then the production of QDs will be increased. Moreover, since the reduction starts after to the addition Na_2S solution, so, if strong magnetic stirring was given while Na_2S solution was added; that could help the produced NPs to be decorated homogeneously on GR sheet. Furthermore, it was also assumed that NPs could grow more in the core of 3D porous rGO structure than the other parts of the body. For this reasons, this whole process was repeated twice, first time 120mg $CdCl_2$ (Fig. 6a step-II) was added instead of 20mg and in this case aggregation started after two hours and after 6 hours it became nice 3D porous structure of rGO. Second time 120mg $CdCl_2$ was added but in this later case strong magnetic stirring was utilized instead of shaking when the Na_2S solution was added (Fig. 6a step-III). In this case aggregation also started after two hours and nice 3D porous structure of rGO was formed after 6 hours. In both cases, some sample was collected from the core and some sample was collected from the other parts of the sample and washed same as before, but each time of washing 5 minutes magnetic stirring was performed.

Method 2 - One-step method with the impact of solvents and cross linkers

In previous method (Method 1) self-assembly of rGO *in situ* in water was examined to produce NPs decorated 3D porous rGO structure. By this method the formation of 3D rGO was very nice, but the decoration of QDs on rGO was not in acceptable (some results are shown in the results section). Therefore, in an attempt to improve this issue the decoration of QDs in 3D rGO was attempted by utilizing a mixture of organic and inorganic solvent, in specific a mixture of water and ethanol (Fig. 6a step-I). Since, a previous study has revealed that benzyl mercaptan (BM) can act as a cross linker between the NPs and GR sheets [49], BM was added in this study to observe the outcome as an anchoring element as well as to observe its effects on the production of 3D rGO structure. 30ml GO water solution (0.001g GO/ml water, 30 minutes strongly sonicated) was taken into a bottle and 30ml C_2H_5OH (99.5 %), 100ml BM (benzyl mercaptan) was added into this bottle (Fig. 6a step-I). 6ml $CdCl_2$ water solution(5mg $CdCl_2$/ml water) (Fig. 6a step-II) and 0.3g Na_2S was added into this bottle (Fig. 6a step-III), shaken the bottle strongly to dissolve Na_2S into the solution and the bottle was kept in the oven for 6 hours at 90°C under atmospheric pressure. In this case it took long time to precipitate and after 4 hours gelation was started. After 6 hours bottle was taken out from the oven, very soft 3D structure of rGO was formed. The sample was washed same as before and each time 5 minutes strong sonictaion was given. After each time of washing sample was collected by performing 10 minutes centrifugation.

Method 3 - One-step method with Cadmium acetate dihydrate instead of $CdCl_2$

In all the previous methods (1, 2) $CdCl_2$ was utilized in a view to produce QDs in the solution and it has been observed that either the decoration of QDs or the formation of 3D rGO structure was not in expected level. Thus, in this study cadmium acetate dihydrate was utilized instead of $CdCl_2$ and its impact on the production of QDs has been observed. 50ml GO solution (0.001g GO/ml water, 1 hour strongly sonicated) was taken into a bottle and 30mg cadmium acetate dihydrate was mixed with this solution and shaken the bottle to dissolve it perfectly (Fig. 6a step-II). 0.3g Na_2S was mixed with 4ml water in another small bottle and shaken the bottle strongly to dissolve it, then this Na_2S solution was added into the first bottle drop by drop at rate of 1 drop/sec under simultaneous shaking (in Fig. 6a step-III). The bottle was then kept in the oven at 90°C under atmospheric pressure, after one and half hour it started to aggregate, 6 hours later bottle was taken out from oven and 3D porous structure of rGO was formed nicely. Sample was washed by similar process as before and each time it was stirred 5 minutes by magnetic stirrer.

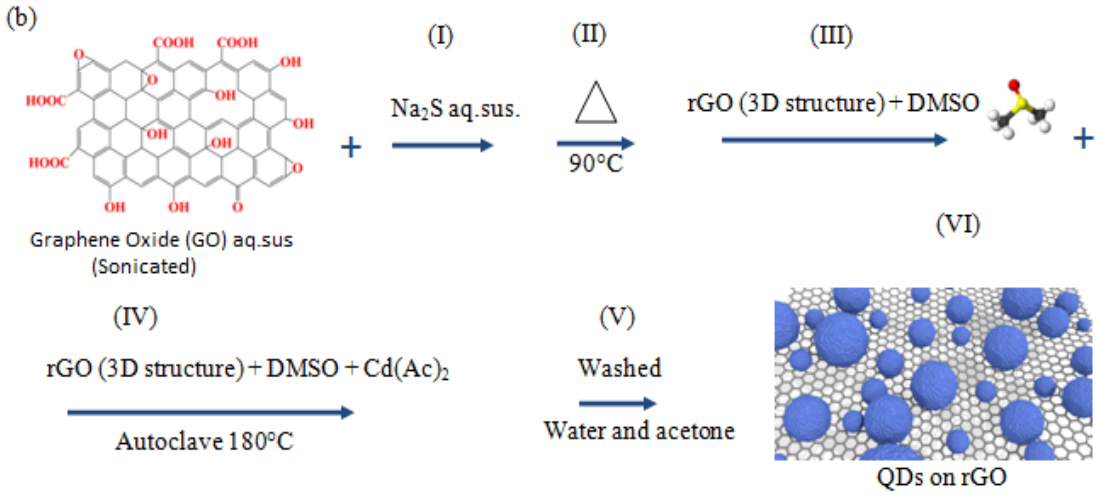

Fig. 6(b) QDs decorated 3D rGO synthesis scheme shows the procedure where 3D rGO was produced separately at the beginning. Later it was tried to decorate QDs in it with help of dimethyl sulfoxide (DMSO) and autoclave method.

Method 4 - Production of 3D rGO separately followed by attaching QDs with the help of DMSO and autoclave

All the previous methods (1, 2, 3) it was tried to produce QDs and anchor them in 3D rGO concurrently at the time of synthesis. However, as already expressed the achieved materials were not in line with expectations. The main issue was that when the decoration of CdS QDs were nice and homogeneous, the produced 3D rGO was too soft and fragile, or vice versa when 3D rGO was nicely porous, yet strong and robust, then the decoration of QDs were not homogeneous or too low. Hence, in this process 3D porous structure of rGO without QDs decoration was prepared initially by the chemical reduction method, and later CdS was attached with rGO sheets in DMSO solvent with the help of an autoclave method. DMSO can be used as solvent and sulfur precursor due to its slow decomposition at high temperature, which is good for decorating CdS QDs onto graphene structure [50]. 60ml GO water solution (0.001g GO/ml water, 30 minutes strongly sonicated) was taken into a bottle. 0.3g Na_2S was mixed with 4ml water in another small bottle and shaken the bottle strongly to dissolve it perfectly. This Na_2S solution was added into the first bottle drop by drop at the rate of 1 drop/sec under simultaneous shaking (Fig. 6b step-I). The bottle was then kept in the oven at 90°C under atmospheric pressure and after two hours it was started to precipitate and getting good shape (Fig. 6b step-II). Bottle was taken out from the oven after 6 hours and 3D porous structure of rGO was formed nicely. The liquid from the bottle was decanted, leaving the 3D structure of rGO. DMSO was poured into this bottle until the 3D structure was fully floating on it. Sample was kept into DMSO several hours and after every 2 hours interval DMSO was changed and new DMSO was poured. This was repeated 4 times and last time sample was kept into DMSO for more than 10 hours and the color of the DMSO was changed, it became little bit blue (Fig. 6b step-III). An autoclave was filled with DMSO and 0.5g cadmium acetate dihydrate was mixed with it. Previously produced 3D rGO structure was kept in the autoclave and then put it at 180 °C for 12 hours (in Fig. 6b step-IV). Sample was washed

three times with water and acetone same as before and collected by performing 10 minutes centrifugation. The result of this method was very good, but a major disadvantage is that the DMSO solution produces a very bad smell when decomposing due to its sulfur content.

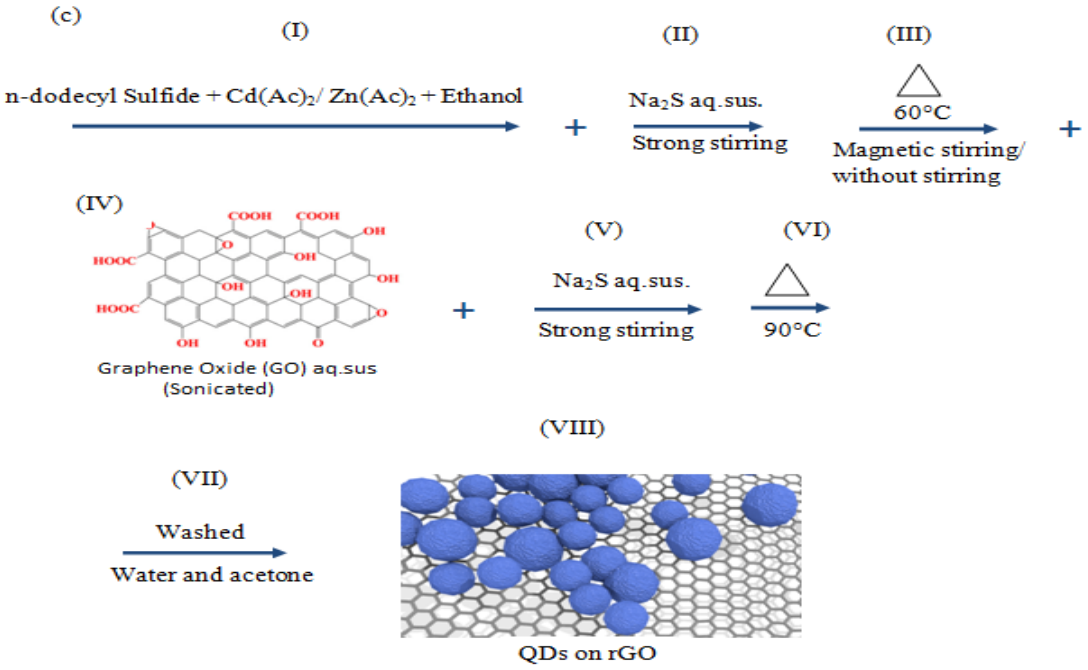

Fig. 6(c) Scheme is showing the synthesis process where QDs were produced separately and later it was tried to decorate them in 3D rGO at the same time of synthesis.

Method 5 - Production of QDs separately followed by attaching them in 3D rGO

Though the decoration of QDs in 3D rGO was good in method 4 but this method produces very unpleasant smell. Therefore, in this approach QDs were produced individually and later it was attempted to attach them in 3D rGO concurrently in the synthesis process. Chen et al [51] reported the anchorage of Pd nanoparticles on carbon nanotubes (CNTs) and they used BM-modified Pd where BM acted as a cross linker between Pd and CNTs. Herein, following the same procedure but without any cross linker, it has been attempted to anchor Cd or Zn nanoparticles instead of Pd on rGO sheets. 0.0185g n-dodecyl sulfide and 0.026g cadmium acetate dihydrate was dissolved into 20ml ethanol (99.5%) (Fig. 6c step-I). Na_2S was dissolved into 1ml water and shaken, this solution was mixed with the solution prepared in Fig. 6c step-1 drop by drop at rate of 1 drop/sec under strong stirring, whole mixture was heated 1 hour at 60°C (Fig. 6c step-III). 60ml GO solution (0.001g GO/ml water, 30 minutes strongly sonicated) was taken into a bottle and 5ml mixture (made in Fig. 6c step-III) was mixed with this solution under strong stirring. 0.3g Na_2S was mixed with 4ml water in another small bottle and shaking the bottle strongly to dissolve it. This Na_2S solution was added into the GO solution drop by drop at dropping speed of 1 drop/sec under strong stirring (Fig. 6c step-V). This whole mixture was kept in oven at 90°C under atmospheric pressure and after 4 hours it started to precipitate and the bottle was kept 20 hours in the oven. The 3D structure was very soft and it was washed three times with water and acetone, and each time it was collected by 10 minutes centrifugation.

Pan et al. [52] reported that if nanoparticles is produced without support of GR, then they stack randomly and agglomerate together, therefore, strong magnetic stirring was given to prevent the agglomeration when the mixture was heated one hour in step-III (Fig. 6c). Furthermore, the decoration of both Cd and Zn nanoparticles on rGO sheets in 3D porous rGO has been observed separately. So, this process was repeated twice in different parameter. First time, in step-III (Fig. 6c) the solution was given strong magnetic stirring when it was heated 1 hour at 60°C. In this case sample also took 4 hours to start aggregation. After 20 hours sample was taken out from the oven, it was very soft 3D structure of rGO. Second time, Zinc acetate dihydrate was added in step-I(Fig. 6c) instead of Cadmium acetate dihydrate and same as before in step-III (Fig. 6c) strong magnetic stirring was given. It did not aggregate even after long time and the sample was taken out from the oven after 18 hours, it was not in nice 3D structure, however, there was precipitation. In both cases sample was washed same as before.

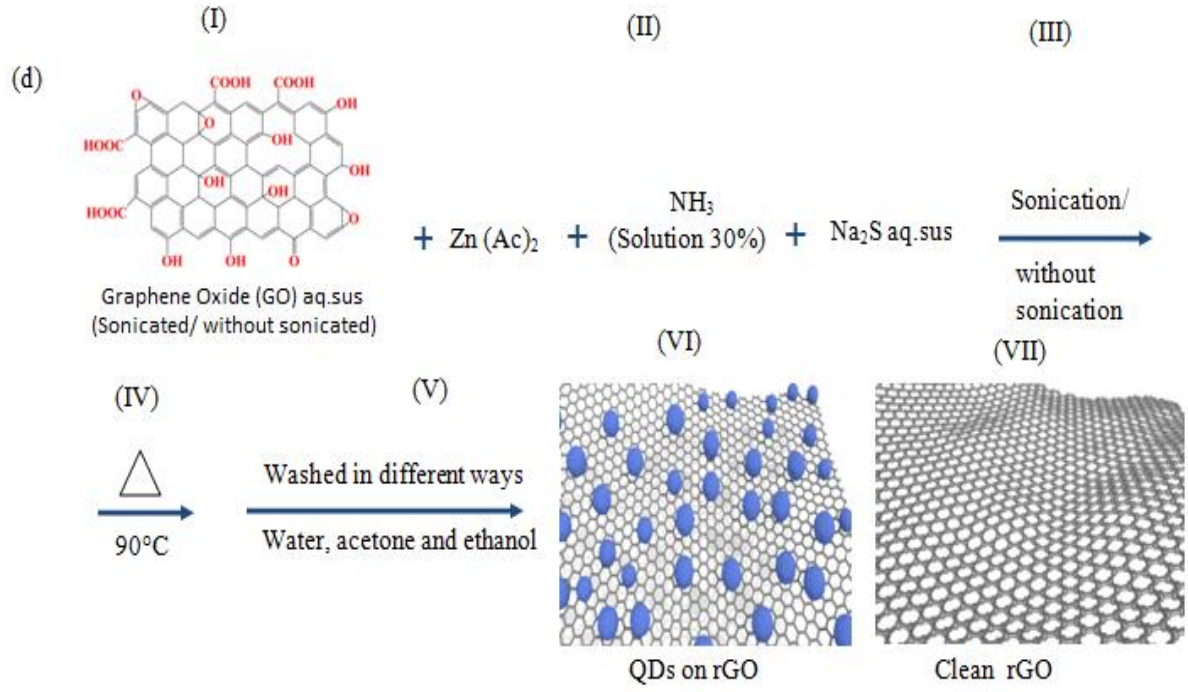

Fig. 6(d) The most successful method to decorate QDs in 3D rGO is visualized in this scheme, where decoration of QDs in 3D rGO and formation of three dimensional structure of rGO happens simultaneously in synthesis.

Method 6 - One-step method with controlling pH values, homogeneous decoration and maintaining mechanical stability

Decoration of QDs in 3D rGO was good in method 5; however, produced 3D structure was very soft. In all approaches have followed so far, it was tried to produce 3D porous rGO decorated with NPs by chemical reduction in solution based process using Na_2S as a reducing agent, and in all approaches GO water solution were given 30 minutes strong sonication at the beginning. However, study report has revealed that the aggregation of rGO can be tuned by

controlling the p^H values [44]. Therefore, in this approach the effect of p^H values in the aggregation of rGO and in the decoration of NPs on rGO has been observed. The effect in the aggregation of rGO; if GO aqueous solution is not given strong sonication at the beginning, and the influence of the amount of reducing agent in the gelation of rGO, as well as the decoration of NPs on rGO in each case has also been observed. 60mg GO and 110mg $Zn(CH_3COO)_2.2H_2O$ were mixed with 60ml water and shaken strongly (In Fig. 6d step-I). To control the p^H value, 165µL ammonia solution (30%) was mixed with this solution and the p^H value was around 8 (In Fig. 6d step-II). 200mg Na_2S was mixed with 10ml water and shaken to dissolve it perfectly, and prepared Na_2S solution was mixed with the mixture prepared earlier drop by drop (1drop/sec) (Fig. 6d step-II). Whole mixture was given 30 minutes strong sonication (Fig. 6d step-III) and the bottle was kept in the oven at 90°C under atmospheric pressure (Fig. 6d step-IV). It took long time to start aggregation but after roughly 6 hours it finally started to aggregate. After 21 hours the bottle was taken out from the oven and the sample was in 3D structure but very soft. Sample was washed three times separately with water and acetone, each time sample was collected by performing 10 minutes centrifugation.

Since in the earlier study the produced 3D rGO was very soft thus, this process was repeated twice in different parameter. First time, GO water solution was given 30 minutes strong sonication at the beginning (Fig. 6d step-I). 300mg Na_2S was mixed with 4ml distilled water and this solution was added drop by drop (1drop/sec) (in Fig. 6d step-II). This time it started to aggregate after one and half hours and after 6 hours sample was taken out from the oven and nice 3D porous structure of rGO was formed. Sample was washed same as before. Second time, GO water solution was given 30 minutes strong sonication at the beginning and 300mg Na_2S was added same as before but in this case, whole mixture was given again 30 minutes strong sonication (in Fig. 6d step-III) before placing in the oven. This time it started to aggregate after one hour and sample was taken out from the oven after 6 hours and nice 3D porous structure was formed. After analyzing the outcome of the various methods used in method 6 it was suspected that the washing solvents might lead to a removal of the decorated NPs from the individual rGO sheets, or that during the washing procedure the NPs tend to agglomerated on certain areas of rGO sheets. To address this issue different washing procedure were investigated (each time the sample was washed for three times) (Fig. 6d step-V), (a) with water and acetone separately, (b) with only water, (c) with only acetone, (d) with the mixture of water and ethanol (99.5%), followed by an analysis of the produced results.

4. Characterization

The most important characteristics of rGO decorated by nanoparticles is to investigate the size distribution, the homogeneity, the anchoring and the overall distribution of the nanoparticles on the reduced graphene oxide surface. To study these properties, the samples were investigated by Transmission Electron Microscopy (TEM: JEOL JEM-1230 transmission electron microscope at 80 keV), and high resolution Transmission Electron Microscopy, HR-TEM (JEM-2100F at 200 keV with a Gatan Imaging Filter). To study the crystalline properties of the NPs, TEM images were used together with electron diffraction. For the TEM investigations samples were dispersed in ethanol (99.5%) by one minute sonication, and a

drop of the solution was put on a copper grid and then dried properly before it was shifted to the TEM sample chamber. To study the macrostructure of the decorated 3D-rGO Field Emission Scanning Electron Microscopes (FE-SEM) was used (Zeiss Merlin FEGSEM, 30kV and a beam current of 210 pA). When sample was investigated by TEM, HRTEM and SEM 15-20 images were investigated for each sample and most representative images are included in this text. The X-ray diffraction (XRD) pattern of the ZnS decorated GR was examined by a D/MAX-RA type powder diffractionmeter (LabX XRD-6000, Shimadzu), with Cu k_α radiation (λ=1.5418Å, voltage 40 kV and current 30 mA).

5. Results and discussions

5.1 High mechanical stability but poor QDs decoration

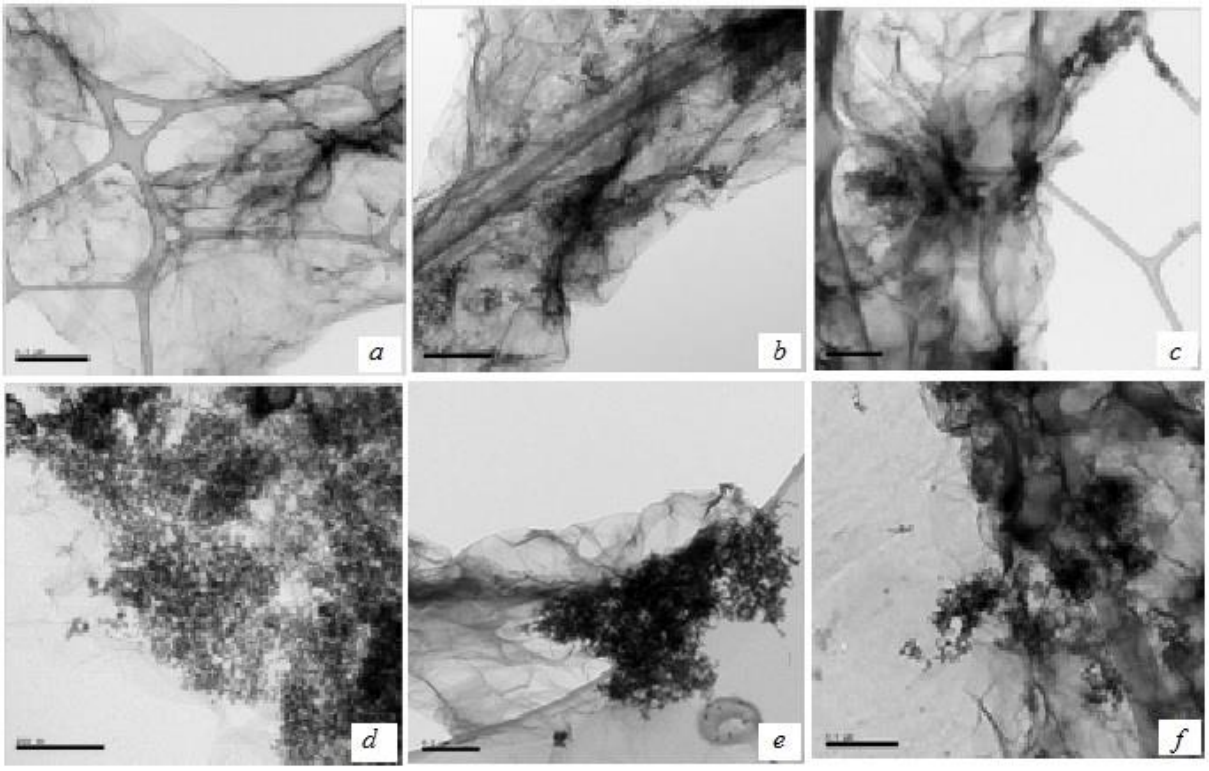

Fig. 7 TEM images of rGO-CdS nanocomposites. Scale bars are *d* 200nm, *e* 0.2µm, and *f* 0.5µm.

It is clear from our experiments, and also in line with expectations, that the amount of NPs on rGO depends on the access of $CdCl_2$, so that the number of CdS NPs on rGO increases when a higher amount of $CdCl_2$ is added to the synthesis process. This is visualized in Fig. 7*a* which shows the TEM image when 10mg $CdCl_2$ was used (in Fig. 6a step-II). It is apparent that this sample is showing the clean rGO and it was more clean when the amount of $CdCl_2$ was lesser than 10mg. The TEM images in Fig. 7*b* and in Fig. 7*c* are showing the decoration of CdS NPs on rGO when 20mg $CdCl_2$ was used (in Fig. 6a step-II). The TEM image in Fig. 7*b* is showing when the sample was given strong magnetic stirring and the TEM image in Fig. 7*c* is showing when the sample was given strong sonication at the time of washing (in Fig. 6a step-

V). It has been found that when 20mg $CdCl_2$ was used; some CdS NPs was produced on rGO though they were agglomerated together on certain area of rGO. It was thought that strong sonication or magnetic stirring might have important role behind the agglomeration of NPs when the sample was washed to remove the unwanted byproducts produced in this reaction. Moreover, it has been found that neither the sonication nor the magnetic stirring at the time of washing can affect the decoration of NPs on rGO. As Na_2S was used as a reducing agent and bottle was kept in the oven at 90°C at normal atmospheric pressure, each time sample started to aggregate after one and half hours. Furthermore, TEM image in Fig. 7*d* shows that suitable number of CdS NPs have grown on rGO when 120mg $CdCl_2$ was used in this reaction (in Fig. 6a step-II). In this case the aggregation of rGO started after slightly longer time (two hours) due to the large amount of NPs produced. It was thought that if magnetic stirring is given when Na_2S solution was added to GO solution (in Fig. 6a step-III), it might help to the homogenous dispersion of NPs on rGO. It was also thought that more NPs might grow at the core of the 3D porous rGO than the other parts. The TEM image in Fig. 7*e* is showing the decoration of CdS NPs on rGO when the sample was collected from all part of the 3D rGO structure. The TEM image in Fig. 7*f* is showing the attachment of CdS NPs with rGO when the sample was collected from the core of 3D rGO architecture. It has been observed that magnetic stirring don't help to homogeneous decoration of NPs on rGO and they grow everywhere irrespective to the core or all part of the 3D rGO.

5.2 QDs decorated in 3D rGO with some other problems

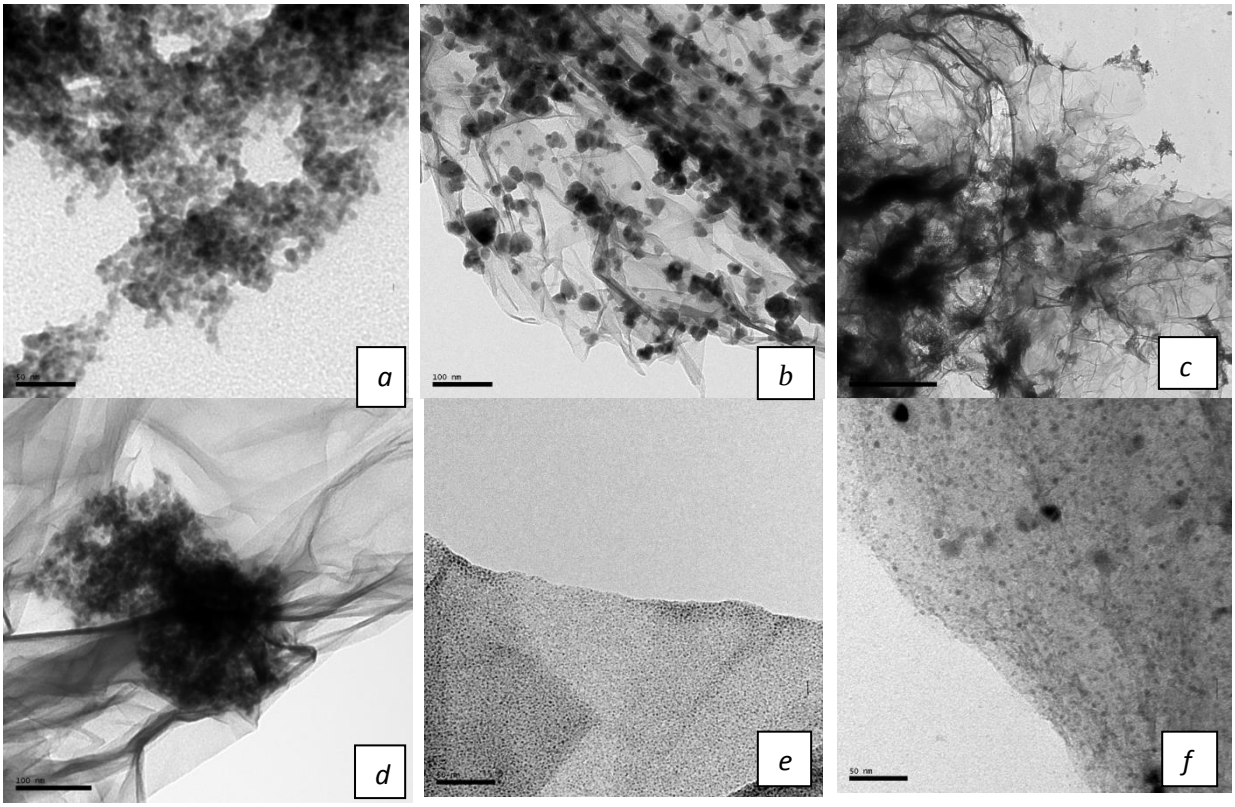

Fig. 8 (*a-f*) TEM images of NPs decorated rGO. Scale bars *a*, *e* and *f* 50nm, *b* and *d* 100nm, *c* 1µm.

TEM image in Fig. 8*a* shows the attachment CdS NPs on rGO sheet when BM was used (in Fig. 6a step-I) as a cross linker between NPs and rGO sheets. This image is showing that there are huge amount of NPs attached on rGO sheets though they are slightly agglomerated. BM was used because the benzene rings in the BM anchor to CdS during formation process, foil the aggregation, interact with rGO via π-π stacking as well as act as a inter linker between the rGO sheets and NPs [49]. In a view to test the effect of different solvent, C_2H_5OH (99.5%) was mixed with water (in Fig. 6a step-I), in consequence the re-stacking of rGO sheet was significantly hindered due to the presence of hydroxyl groups of the ethanol. It was noticed that when GO sheets was reduced, their basal planes became hydrophobic becasue of the elimination of hydroxyl and epoxy groups and restroing conjugated domains, which helps to a three dimensional arbitrary stacking between flexible graphene sheets. However, introduction of ethanol increases the repulsion forces between the graphene sheets. As a result, aggregation was started after four hours and 3D structure of rGO was very soft even after six hours. On other hand, this repulsion force makes space for NPs to sit on rGO sheets.

In Fig. 8*b* TEM image indicates that a lot of CdS NPs are attached on rGO when DMSO was utilized (in Fig. 6b step-IV) in autoclave method. In this TEM image it has been noticed that the produced NPs are dispersed uniformly on rGO sheets, however, they are a bit big in size around 10-20nm. When 3D porous structure of rGO was dipped into DMSO (in Fig. 6b step-III), here it played an important role as a solvent as well as a source of sulfur [50]. Moreover, when the sample was taken out from the autoclave, it has been found that this process produce very bad smell due to the abundant sulfur source, so special treatment can be applied or mask can be used in this process. Since we aim for a synthesis process that should be possible to implement in ordinary lab environment we choose to not test this method further, despite the promising results. The TEM image in Fig. 8*c* shows that cluster of CdS NPs on rGO when GO aqueous solution was given 1 hour sonication (in Fig. 6a step-I) and 30mg cadmium acetate dihydrate was used (in Fig. 6a step-II) instead of $CdCl_2$.

When Chen et al. [51] procedure was followed but any cross linker was not used, the TEM image in Fig. 8*d* is exhibiting that CdS NPs are anchored on rGO sheets but they are agglomerated together. The TEM image in Fig. 8*e* is showing that CdS NPs are decorated on rGO by utilizing magnetic stirring in step-III (Fig. 6c). As seen from the TEM image the NPs are very homogeneously dispersed on rGO and NPs sizes are around 2-3nm. The TEM image in Fig. 8*f* is demonstrating that ZnS NPs are attached uniformly on rGO when magnetic stirring was given in step-III (Fig. 6c). Furthermore, this TEM image also indicates that around 2-3nm sized NPs are homogeneously decorated on rGO. Since ethanol (99.5%) was used in each attempt, so due to the ample hydroxyl groups the repulsion force between rGO sheets were increased, thus each time it took long time to start gelation and 3D structure of rGO was very soft. Moreover, when zinc acetated dihydrate was used then 3D structure of rGO was not formed though there was precipitation of rGO. In this case a lot of NPs are produced and they might also increase the repulsion force between the rGO sheets.

5.3 Homogeneous decoration of QDs in 3D rGO with high mechanical stability

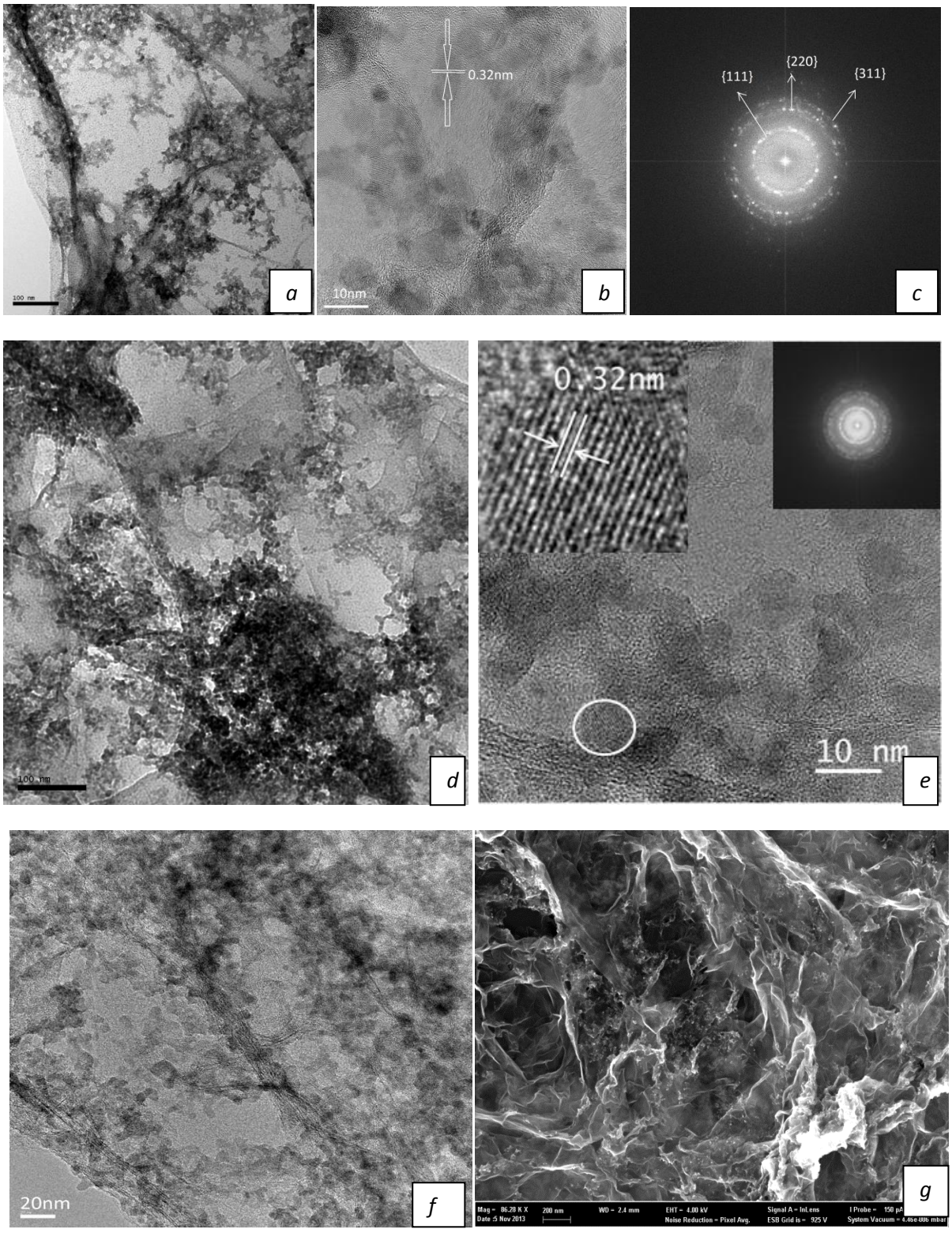

Fig. 9 TEM (*a, d*) and HRTEM (*b, e, f*) images of ZnS NPs-rGO nanocomposites; the inset in *e* and *c* are FFT pattern of the composite. SEM (*g*) images of ZnS NPs-rGO nanocomposites. Scale bars *a* and *d* 100nm, *g* 200nm.

Each time of synthesis GO water solution was given strong sonication before adding any chemicals, which helps to get GO nanosheets suspension in water where individual GO flakes are stabilized due to the mutual electrostatic attraction and repulsion. Nevertheless, one attempt has been taken when GO water solution was not given sonication at the beginning and less amount of reducing agent was used. TEM image in Fig. 9*a* is showing that a lot of ZnS NPs are attached on rGO sheets and their sizes are around 4-5nm and they are homogenously dispersed on rGO sheets. High resolution TEM image in Fig. 9 *b* is also revealing the ZnS NPs equipped rGO sheets where NPs are well dispersed on it and their sizes are around 4-5nm. Study reported that p^H has significant impact on the gelation of additive free GO, thus p^H was maintained around 8 in this attempt and 30 minutes strong sonication was given (in Fig. 6d step-III) after adding all the chemicals. It has been found that aggregation started after 6 hours and even after 21 hours very soft 3D rGO shape was formed because the repulsion force between the graphene sheets were increased due to the high p^H value. Moreover, π-π interaction between the rGO sheets was not very strong compared to the repulsion force and the rGO sheets was less hydrophobic due to the addition of less amount (200mg) of reducing agent. Both these facts have played key role behind the delayed aggregation. Furthermore, as the GO water solution was not given strong sonication before adding any chemicals the particular GO flakes were not stabilized and well dispersed in water which further retarded the aggregation of rGO. We also noted that the repulsion force between the rGO sheets which is originated by the high p^H value paves way for the NPs to take position on rGO sheets and attach with it.

This method was further modified to study the influence of sonication in GO water solution and the effect of the reduction. The same steps as before were used but here the solution was given 30 minutes strong sonication (in Fig. 6d step-I) before adding any chemicals and the amount of reducing agent was increased (300mg). The results are shown in the TEM image in Fig. 9*d*, which displays that a lot of ZnS semiconductor NPs are homogeneously dispersed on rGO sheets with sizes around 4-5nm. It has also noted that, in this step aggregation of rGO was started after one and half hours and after 6 hours the 3D shape of rGO was formed, whereas in earlier case when strong sonication was not given at the beginning, it took 6 hours to start aggregation and even after 21 hours 3D shape was very soft.

Compton et al. [45] reported that ultrasonication facilitate the aggregation of pure GO. To test this, another approach has been considered where GO water solution was given 30 minutes strong sonication (In Fig. 6d step-I) before adding any chemical followed by a subsequent 30 minutes strong sonication (in Fig. 6d step-III) to the whole mixture after adding all chemicals. As a consequence, it was found that aggregation started after one hour and after 6 hours nice 3D porous rGO structure was formed. The high resolution TEM images of these samples are shown in Fig. 9*e* and in Fig. 9*f* and display that the ZnS semiconductor NPs decorated on rGO are around 4-5nm and that the NPs are uniformly dispersed on rGO sheets. As the amount of reducing agent was increased in these both studies hence, the GO flakes became more hydrophobic and the π-π interaction between the rGO sheets are increased, for these reasons the aggregation of rGO was prompted. Since the strong sonication breaks GR sheets and which destabilize the existing carboxyl groups and also change the surface chemistry, so

alongside with reduction sonication also have significant impact on aggregation of rGO. Moreover, there is a small repulsion force between the rGO sheets due to the high p^H value though it is not stronger than the attractive force produced due to the reduction, and this small repulsion force helps the NPs to occupy their position nicely on rGO sheets as well as anchor with it.

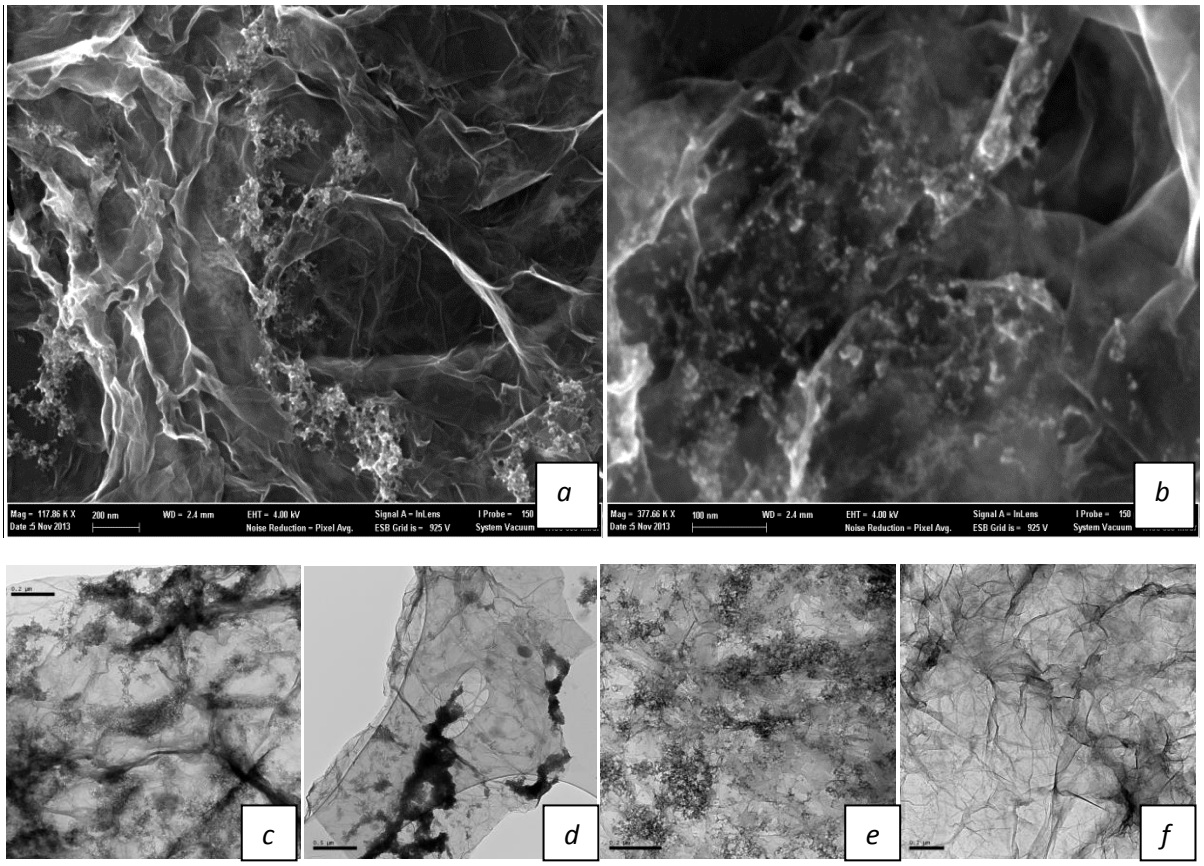

Fig. 10 TEM (*c*, *d*, *e*, *f*), and SEM (*a*, *b*) images of ZnS NPs decorated rGO. Scale bars *a* 200nm, *b* 100nm, *c* 0.2µm, *d* 0.5µm, *e* and *f* 0.2µm.

5.4 Impact of washing solvent on NPs decorated GR sheets

Throughout the work of entire thesis, after each time of synthesis the produced 3D rGO was washed three times with water and acetone separately to purify the rGO and to remove the unwanted byproducts. To investigate the effect of washing procedure we have investigated the same sample before and after washing. This is visualized by comparing two TEM images in Fig. 9*d* and in Fig. 10*c*. Though these two images are showing the attachment of semiconductor NPs on rGO when the sample was collected from the same 3D rGO, it is clear that the decoration of NPs on rGO is very different. In addition, high resolution TEM image in Fig. 9*f* is also showing that rGO sheets are decorated by relatively well distributed semiconductor NPs while the TEM image in Fig. 10*c* shows that the NPs have agglomerated into chains or islands. By comparing the TEM images in Fig. 10*c* and 9*f* it can also be seen that the rGO might be slightly damaged after being washed with water and acetone, which can further expose the decorated semiconductor NPs to the washing solvent. As a result, either the semiconductor NPs attached on rGO were dissolved into the washing solvent or the washing solvent has weakened their attachment force, which causes them to be agglomerated on

certain region of rGO sheets. To test this hypothesis the sample was divided into several parts and some part of the same sample was washed three times only with acetone to observe the effect of it on NPs decoration on rGO. The TEM image in Fig. 10*d* is showing the decoration of NPs on rGO after washing it with acetone. From this image one can notice that the NPs which were earlier uniformly decorated on rGO now are either dissolved into the acetone or acetone has weakened the anchoring force between the semiconductor NPs and rGO sheets. As a consequence, most of the region of rGO sheets are unoccupied by semiconductor NPs and huge cluster of NPs are situated on particular area of rGO sheets.

Furthermore, to study the impact of water as a washing solvent on semiconductor NPs decorated rGO, some part of the same sample of 3D rGO was washed three times only with water. In this case in Fig. 10*e* the TEM image indicates that a lot of semiconductor NPs are still attached on rGO sheets and most of its areas are occupied by 4-5nm sized NPs. To perform detailed morphological analysis of the sample, scanning electron microscopy (SEM) photographs were taken when the sample was washed with different washing solvent. When the sample was washed with only water, the SEM images in Fig. 9*g* and in Fig. 10*b* are showing that plenty of semiconductor NPs are uniformly attached on the rGO sheets and they are not clustered together. On the other hand when the same sample was washed with water and acetone, the SEM image in Fig. 10*a* reveals that semiconductor NPs are attached on rGO however, there are little cluster of NPs on it. It is not easy to remove all the byproducts by using water as washing solvent, so in another approach some part of the sample was washed three times with the mixture of water and ethanol (99.5%) to purify it perfectly. The TEM image in Fig. 10*f* is indicating the totally clean rGO sheets and semiconductor NPs are not attached on it, because either the attached NPs are dissolved into the mixture of water and ethanol completely or this mixture has entirely broken the anchoring force between the NPs and rGO. In addition, ethanol contains hydroxyl groups, thus the excess hydroxyl groups increases the repulsion force between the adjacent rGO sheets which might support the NPs to be dissolved into the washing solvent smoothly.

5.5 Mechanical strength and porosity of NPs decorated 3D rGO

Mechanical strength of the NPs decorated 3D rGO produced in this process depends on many factors, out of them three factors such as amount of reducing agent, giving sonication to GO aqueous suspension and the solvent (which is used in the synthesis process) have been clearly identified. When 0.3g Na_2S was used as reducing agent in Fig. 6a step-III and strong sonication was given to the GO aqueous solution at the beginning, then 3D rGO was formed with good mechanical strength. Produced 3D rGO was given strong shaking with water and acetone during the washing time, this strong shaking was not able to break the 3D structure of rGO. It has been also noticed that formed 3D rGO could support the weight many times higher than its own weight. Moreover, in another approach it has been also confirmed that by controlling the amount of reducing agent and utilizing sonication to GO aqueous solution the mechanical strength of 3D rGO can be controlled. In Fig. 6d step-I when GO water solution was not given strong sonication at the beginning and in step-II 0.2g Na_2S was used as reducing agent then mechanical potency of the produced 3D rGO was not good enough. On the other hand in the same approach when in step-II 0.3g Na_2S was used and strong sonication

was given in step-I as well as in step-III, then 3D rGO with high mechanical strength was formed. This produced 3D structure of rGO was given strong shaking with different solvent such as water, acetone, and mixture of water and ethanol during the washing nevertheless, it has been observed that 3D structure of rGO was not breaking easily even after strong shaking. Hydroxyl groups increase the repulsion forces between the individual rGO sheets which significantly hamper the mechanical strength of the produced 3D rGO and it has been ensured in several approaches. In Fig. 6a step-II when ethanol was used with water as a solvent then formed 3D rGO was very soft. This effect has been clearly observed in Fig. 6d step-V when sample was washed with the mixture of water and ethanol. The negative impact of ethanol on the mechanical strength of produced 3D rGO has also been confirmed in Fig. 6c step-I. Same as before, ethanol was used in this step and in consequence, produced 3D rGO was very soft.

It is mentioned earlier that the attraction force between the rGO sheets increases due to the reduction. This attraction force leads rGO sheets re-stacking to form three dimensional structure of rGO. However, during the re-stacking rGO sheets cannot sit one upon another to form a tightly packed 3D structure, because some rGO sheets take position vertically in between two other rGO sheets. As the individual rGO sheet has strong mechanical strength, therefore this rGO sheet which is placed vertically in between two other sheets can make free space or gap in between the rGO sheets. Moreover, rGO sheets are not perfect planes and some of them are wrinkled. This is how a lot of micro sized pores and inter connected channels are produced in 3D rGO. The SEM images (in Fig. 9*g*, 10*a*, 10*b*) show that there are a lot of micro pores and inter connected channels are available between the reduced rGO sheets. It has been also noticed in these SEM images that a lot of NPs are attached with reduced rGO sheets and many NPs are uniformly dispersed and entrapped in between reduced rGO sheets. The NPs also make gap between reduced rGO sheets, which helps to produce interconnected network in 3D rGO.

5.6 Confirmation of ZnS QDs on rGO

Herein, crystalline nature has been explained by using the high resolution TEM images and fast-Fourier transform patterns. The high resolution TEM images in Fig. 9*b*, and in Fig. 9*e* indicate the lattice fringes of the nanocrystals with interplanar distance of 0.32nm which corresponds well with the (111) plane of zinc blende ZnS. The fast-Fourier transform (FFT) pattern in Fig. 9c and the inset in Fig. 9*e* clearly show three inner diffraction rings which can be assigned as diffraction from (111), (220) and (311) planes of ZnS nanoparticles [53]. Furthermore, x-ray diffraction (XRD) was carried out and the diffraction peaks could be well indexed to originate from the (111), (220) and (311) crystal planes of zinc blende ZnS respectively. The observed x-ray diffraction peaks of the bulk sample is however complicated by the presence of diffraction peaks originating from metal salts remaining as impurities in the sample. Therefore the indexing is more reliable made from electron diffraction patterns obtained by the electron microscopy.

6. Applications of QDs decorated 3D rGO

Since inter linker has not been used in this process when semiconductor NPs were decorated on rGO sheets or semiconductor NPs were not modified by any cross linker before the

synthesis, so any shell or cap was not build around the NPs which can make barrier for the excited electron or hole to reach the acceptor (GR). By virtue of the fast generation of electron-hole pairs by photo-excitation and the highly negative reduction potential of the excited electron, ZnS NPs is considered as a good photocatalysts [54]. Moreover, ZnS NPs are decorated on rGO and they are dispersed on it uniformly, and they are placed in between the rGO sheets, so when electron is excited by photon it can be easily collected by rGO (acceptor). This mechanism of fast electron separation and transportation help in building an efficient solar cell. In addition, as the produced QDs decorated 3D rGO is porous, and a lot of inter-connected channels and networks are available, it can be assumed that if 3D rGO is sliced into appropriately thin slices, it would be semi-transparent or transparent (depending on thickness) which could help to harvest the sun efficiently further down into the photovoltaic device. Furthermore, to increase the efficiency of this solar cell it is very important to remove all the byproduct therefore, produced 3D porous ZnS-rGO can be purified several times by dry freeze method and it can be immersed into water for long time and water could be changed after certain interval. Following different ways, semiconductor NPs decorated 3D porous rGO might be applied effectively in various fields [8, 55], such as nanoelectronics [43, 56], intercalation materials [56], catalysis [43], drug distribution [43, 57], biosensor [43, 58], polymer hybrids [59] and supercapacitors [43, 59].

7. Conclusions and perspectives

In summary, ZnS QDs decorated 3D structure of rGO was prepared by using GO nanosheets *via* chemical reduction in hydrothermal approach and an *in situ* self-assembly. The process is carried out at 90°C in vacuum oven under atmospheric pressure, which makes it promising to prepare QDs decorated 3D rGO on a large scale. This synthetic process was easy and fast, and it may be extended to the synthesis of other QDs decorated 3D rGO composite. It was revealed that QDs decorated 3D rGO not only have the inherent properties of GR, but also show excellent functions resulting from their exclusive microstructure. This 3D rGO build GR nanosheets into macroscopic materials for practical applications. In this thesis work, after each time of synthesis produced QDs decorated rGO was washed with water and acetone, and at the end it has been found that acetone plays very negative role on the decoration of QDs on rGO. Furthermore, at each time preparing TEM grids ethanol was utilized as a solvent and at the final stage it was found that ethanol also plays a very negative role on the decoration of QDs on rGO. When QDs decorated 3D rGO was washed with a mixture of water and ethanol, it was found that all QDs were removed from the rGO sheets, thus making it very "clean".

Though it was found that the decoration of QDs on rGO is good and homogeneous, it is also clear that some early decoration processes probably were better that what we assumed since utilizing ethanol to prepare the TEM grid and acetone (used to wash the samples) partly dissolved the anchored NPs. Therefore, future studies are needed to optimize the washing procedure to purify QDs decorated 3D rGO without destroying the decoration of QDs. In this study it was also found that the mechanical strength of the produced QDs decorated 3D rGO varies with the synthesis process and the amount of reducing agent as well. Due to the unique microstructure and other properties this QDs decorated 3D rGO can be applied in various

important fields. Further research is strongly recommended to improvement mechanical properties of QDs decorated 3D architecture of rGO.

Acknowledgement

First and foremost, I would like to say " All praise to Allah" who gave me the strength and good health to complete this thesis. My warmest appreciation to my wonderful supervisors Thomas Wågberg and Guangzhi Hu. I appreciate your valuable guidance, advice, insightful comments on my work and helping me to bring it up to the necessary standard for the completion of my thesis. I would like to express my deepest appreciation to all the members in this research group especially Tiva, Hamid and Eduardo for their practical help, sympathy, and their kind welcome to me in so many ways. My sincere thanks also go to Nahid, Musleh, Habib, Pavel, Lincoln and Godwin who helped me in many ways.

8. References

[1] H. Chae, D. Siberio-Perez, J. Kim, Y. Go, M. Eddaoudi, A. Matzger, M. O'Keeffe, O. Yaghi, Nature, 427 (2004) 523-527.
[2] K. Novoselov, A. Geim, S. Morozov, D. Jiang, Y. Zhang, S. Dubonos, I. Grigorieva, A. Firsov, Science, 306 (2004) 666-669.
[3] P. Avouris, Z. Chen, V. Perebeinos, Nature Nanotechnology, 2 (2007) 605-615.
[4] P. Wang, T. Jiang, C. Zhu, Y. Zhai, D. Wang, S. Dong, Nano Research, 3 (2010) 794-799.
[5] D. Chen, L. Tang, J. Li, Chemical Society Reviews, 39 (2010) 3157-3180.
[6] M. Stoller, S. Park, Y. Zhu, J. An, R. Ruoff, Nano Letters, 8 (2008) 3498-3502.
[7] P. Ang, W. Chen, A. Wee, K. Loh, Journal of the American Chemical Society, 130 (2008) 14392-+.
[8] A. Geim, K. Novoselov, Nature Materials, 6 (2007) 183-191.
[9] V. Yong, J. Tour, Small, 6 (2010) 313-318.
[10] X. Zhao, S. Zhou, L. Jiang, W. Hou, Q. Shen, J. Zhu, Chemistry-a European Journal, 18 (2012) 4974-4981.
[11] M. Zeng, W.L. Wang, X.D. Bai, Chinese Physics B, 22 (2013).
[12] Y. Tao, M. Endo, K. Kaneko, Journal of the American Chemical Society, 131 (2009) 904-+.
[13] X. Gui, A. Cao, J. Wei, H. Li, Y. Jia, Z. Li, L. Fan, K. Wang, H. Zhu, D. Wu, Acs Nano, 4 (2010) 2320-2326.
[14] D. Futaba, K. Hata, T. Yamada, T. Hiraoka, Y. Hayamizu, Y. Kakudate, O. Tanaike, H. Hatori, M. Yumura, S. Iijima, Nature Materials, 5 (2006) 987-994.
[15] M. Worsley, S. Kucheyev, J. Satcher, A. Hamza, T. Baumann, Applied Physics Letters, 94 (2009).
[16] J. Trancik, S. Barton, J. Hone, Nano Letters, 8 (2008) 982-987.
[17] M. Shannon, P. Bohn, M. Elimelech, J. Georgiadis, B. Marinas, A. Mayes, Nature, 452 (2008) 301-310.
[18] X. Gui, J. Wei, K. Wang, A. Cao, H. Zhu, Y. Jia, Q. Shu, D. Wu, Advanced Materials, 22 (2010) 617-+.
[19] A.J. Nozik, M.C. Beard, J.M. Luther, M. Law, R.J. Ellingson, J.C. Johnson, Chemical Reviews, 110 (2010) 6873-6890.
[20] A. Zhou, W. Sheng, European Physical Journal B, 68 (2009) 233-236.
[21] Z. Han, Z. Tang, P. Li, G. Yang, Q. Zheng, J. Yang, Nanoscale, 5 (2013) 5462-5467.
[22] S. Mann, Nature Materials, 8 (2009) 781-792.
[23] W. Chen, L. Yan, Nanoscale, 3 (2011) 3132-3137.
[24] Y. Xu, G. Shi, Journal of Materials Chemistry, 21 (2011) 3311-3323.
[25] L. Qiu, J. Liu, S. Chang, Y. Wu, D. Li, Nature Communications, 3 (2012).
[26] X. Huang, X. Qi, F. Boey, H. Zhang, Chemical Society Reviews, 41 (2012) 666-686.

[27] Y. Xu, K. Sheng, C. Li, G. Shi, Acs Nano, 4 (2010) 4324-4330.
[28] M. Matsumoto, S. Saito, I. Ohmine, Nature, 416 (2002) 409-413.
[29] L. Jarup, A. Akesson, Toxicology and Applied Pharmacology, 238 (2009) 201-208.
[30] A. Lerf, H. He, M. Forster, J. Klinowski, Journal of Physical Chemistry B, 102 (1998) 4477-4482.
[31] W. Gao, L. Alemany, L. Ci, P. Ajayan, Nature Chemistry, 1 (2009) 403-408.
[32] L.B. Casablanca, M.A. Shaibat, W.W.W. Cai, S. Park, R. Piner, R.S. Ruoff, Y. Ishii, Journal of the American Chemical Society, 132 (2010) 5672-5676.
[33] D. Li, M. Muller, S. Gilje, R. Kaner, G. Wallace, Nature Nanotechnology, 3 (2008) 101-105.
[34] X. Yang, J. Zhu, L. Qiu, D. Li, Advanced Materials, 23 (2011) 2833-+.
[35] R. Edwards, K. Coleman, Nanoscale, 5 (2013) 38-51.
[36] C. Li, G. Shi, Nanoscale, 4 (2012) 5549-5563.
[37] P. Sutter, J. Flege, E. Sutter, Nature Materials, 7 (2008) 406-411.
[38] K. Kim, Y. Zhao, H. Jang, S. Lee, J. Kim, J. Ahn, P. Kim, J. Choi, B. Hong, Nature, 457 (2009) 706-710.
[39] N. Liu, L. Fu, B. Dai, K. Yan, X. Liu, R. Zhao, Y. Zhang, Z. Liu, Nano Letters, 11 (2011) 297-303.
[40] Y. Hernandez, V. Nicolosi, M. Lotya, F. Blighe, Z. Sun, S. De, I. McGovern, B. Holland, M. Byrne, Y. Gun'ko, J. Boland, P. Niraj, G. Duesberg, S. Krishnamurthy, R. Goodhue, J. Hutchison, V. Scardaci, A. Ferrari, J. Coleman, Nature Nanotechnology, 3 (2008) 563-568.
[41] S. Park, R. Ruoff, Nature Nanotechnology, 5 (2010) 309-309.
[42] D. Dreyer, S. Park, C. Bielawski, R. Ruoff, Chemical Society Reviews, 39 (2010) 228-240.
[43] H. Bai, C. Li, G. Shi, Advanced Materials, 23 (2011) 1089-1115.
[44] H. Bai, C. Li, X. Wang, G. Shi, Journal of Physical Chemistry C, 115 (2011) 5545-5551.
[45] O. Compton, Z. An, K. Putz, B. Hong, B. Hauser, L. Brinson, S. Nguyen, Carbon, 50 (2012) 3399-3406.
[46] A. Nozik, Chemical Physics Letters, 457 (2008) 3-11.
[47] A. Nozik, Physica E-Low-Dimensional Systems & Nanostructures, 14 (2002) 115-120.
[48] J. Blackburn, R. Ellingson, O. Micic, A. Nozik, Journal of Physical Chemistry B, 107 (2003) 102-109.
[49] M. Feng, R. Sun, H. Zhan, Y. Chen, Nanotechnology, 21 (2010).
[50] A. Cao, Z. Liu, S. Chu, M. Wu, Z. Ye, Z. Cai, Y. Chang, S. Wang, Q. Gong, Y. Liu, Advanced Materials, 22 (2010) 103-+.
[51] L. Chen, G. Hu, G. Zou, S. Shao, X. Wang, Electrochemistry Communications, 11 (2009) 504-507.
[52] S. Pan, X. Liu, New Journal of Chemistry, 36 (2012) 1781-1787.
[53] Y.P. Zhu, J. Li, T.Y. Ma, Y.P. Liu, G.H. Du, Z.Y. Yuan, Journal of Materials Chemistry A, 2 (2014) 1093-1101.
[54] J. Hu, L. Ren, Y. Guo, H. Liang, A. Cao, L. Wan, C. Bai, Angewandte Chemie-International Edition, 44 (2005) 1269-1273.
[55] A. Geim, Science, 324 (2009) 1530-1534.
[56] P. Kamat, Journal of Physical Chemistry Letters, 1 (2010) 520-527.
[57] X. Li, X. Wang, L. Zhang, S. Lee, H. Dai, Science, 319 (2008) 1229-1232.
[58] S. Guo, S. Dong, Chemical Society Reviews, 40 (2011) 2644-2672.
[59] C. Rao, A. Sood, K. Subrahmanyam, A. Govindaraj, Angewandte Chemie-International Edition, 48 (2009) 7752-7777.